Indian Journal of Fibre & Textile Research
Vol. 49, December 2024, pp. 416-422
DOI: 10.56042/ijftr.v49i4.3971

Impact of moisture content and thermal exposure on the thermal protective performance of multilayered thermal liner

Tathagata Das[a], Apurba Das & R Alagirusamy
Department of Textile and Fibre Engineering, Indian Institute of Technology Delhi, New Delhi 110 016, India

Received 13 July 2023; revised received and accepted 9 October 2024

This study evaluates the heat transfer index (HTI_{24}) of a multi-layer thermal liner subjected to varying degrees of heat flux under radiant, flame, and 50 % radiant – 50 % flame exposure using a vertical thermal protective performance tester. A three-layer needle-punched nonwoven thermal liner with moisture levels of 0 %, 25 %, 50 %, 75 %, and 100 % is tested across heat flux levels (20, 30 and 40 kW/m^2). Regression analysis identifies the relationship among the heat transfer index, moisture percentage in the thermal liner, and heat flux under different exposure types, with regression equations developed to calculate the HTI_{24} values. Moisture positively influences HTI_{24} during different flame exposures. However, at lower levels of radiative heat flux, water percentage increases the HTI_{24} value, while at higher levels, water percentage has an adverse impact on the HTI_{24} value. These findings highlight the complex interplay of moisture percentage and thermal conditions in optimizing thermal protective performance.

Keywords: Heat transfer index, Moisture percentage, Thermal hazard, Thermal liner, Thermal protective clothing

1 Introduction

Fire hazards pose a serious threat to human life and modern civilization. According to NFPA, 1.35 million fire incidents occurred in the US in 2021, resulting in 3,800 deaths, 14,700 injuries, and $15.9 billion in property damage. Structural fires, which account for more than one-third of all fire incidents, caused the majority of losses, including 3,010 civilian fire deaths (79 %), 12,600 civilian fire injuries (86 %), and $12.7 billion in direct property damage (80 %)[1].

Firefighters play a critical role in minimizing losses caused by such incidents, often risking their lives to protect others. To ensure their safety, firefighters wear thermal protective clothing designed to minimize burn injuries. A typical thermal protective clothing comprise of three layers: outer shell, moisture barrier, and thermal liner. The outer shell limits the flame hazard and wear, the moisture barrier protects against vapour and hot liquids, and the thermal liner acts as a thermal barrier, limiting heat transfer. The European Standard EN 469:2005 outlines the minimal features of firefighter protective clothing across Europe. Firefighters working near fire hazards often encounter conditions where their protective clothing becomes wet due to exposure to water from fire hoses or perspiration. During firefighting, a firefighter can sweat at a rate of 1200 to 1800 g/h^2. Under normal firefighting conditions, almost 75 % of this moisture remains trapped within the garment layers[3,4]. This accumulated water significantly influences heat transfer through thermal protective clothing. It alters the thermal characteristics of the clothing, like heat capacity and thermal conductivity[4,5]. Moisture generally increases the thermal conductivity of the fabric, impairing its thermal protection[6-8]. However, studies also show that moisture can improve thermal protective performance under specific conditions. For example, moisture positively affects thermal protection at low heat flux levels[9], and higher moisture content enhances protective performance in firefighter turnout systems[10]. Further studies reported that for Nomex IIIA woven fabric, the thermal protective performance (TPP) rating increases with water content[11,12]. Fu *et al.*[13] found that for multi-layer thermal protective clothing systems under radiant heat exposure, the temperature increment of different layers of the clothing system is lower in wet state than in dry condition.

The type and intensity of heat exposure also affect thermal protective performance. Fire hazards such as wildfire, structural fires, vehicle fires, and liquefied natural gas (LNG) fires expose firefighters to a wide range of temperatures and heat fluxes[14-17], from

[a]Corresponding author.
E-mail: tathagatadas55@gmail.com

60–200 kW/m² and the temperature up to 1700 °C in structural fires[18] to up to 150 kW/m² with a temperature of 600 °C in wildfires[19]. In vehicle fires, the temperature can rise to 1000℃, although the heat flux remains between 60-80 kW/m^2 [20]. Researchers have categorized firefighting conditions into routine, hazardous, and emergency levels[13,21-24], with heat flux ranging from 2 kW/m^2 for the routine condition to 12.56 kW/m^2 for the hazardous condition to 209.34 kW/m^2 for the emergency condition[24]. Heat flux intensity negatively impacts the time to second-degree burns[25,26]. Lee and Barker[9] reported that at 20 kW/m^2 heat flux, wetted single-layer Kevlar/PBI fabrics provided a higher TPP rating than 84 kW/m^2.

Numerous studies have examined the impact of heat exposure types, such as radiant, flame, and combined convective-radiant heat, on the protective performance of firefighter apparel[27]. Generally, flame exposure offers higher protection compared to radiant heat[28,29]. However, the combined effect of moisture percentages and incident heat flux under different heat exposures on the thermal protective performance of a thermal line remains underexplored. This study evaluates the impact of water content in a multi-layer thermal liner on its protective performance under radiant, flame, and 50 % radiant – 50 % flame exposure. This research measures HTI_{24} for each sample and performs regression analysis to explore the relationship between HTI_{24}, moisture percentages, and heat flux for each heat exposure type.

2 Materials and Methods

2.1 Materials

A thermal liner made of three-layer Nomex IIIA needle punch nonwoven fabric with an areal density of 200 g/m^2 was used in this study (Fig. 1 & Table 1). The nonwoven fabric was made from 38 mm Nomex IIIA staple fibre with a linear density of 1.5 denier. Nomex IIIA nonwoven fabric was selected due to its high Limiting Oxygen Index (LOI) value (28-31%) and exceptionally high degradation temperature.

The nonwoven fabrics were produced using a two-step method. In the first stage, the Trytex carding machine was used to produce Nomex IIIA fibre webs with the specified areal density. These fibre webs were then needle punched in the second phase using a DILO needle punch nonwoven machine. The needle-punching parameters were set to 50 punches/cm² with a penetration depth of 5 mm, yielding a nonwoven fabric with an areal density of 66 g/m².

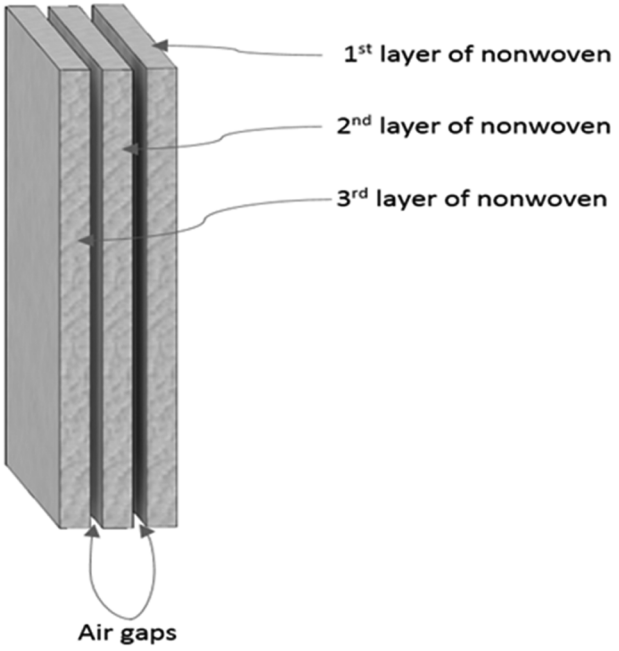

Fig. 1 — Layered structure of the test thermal liner

Table 1 — Physical and thermal properties of the test thermal liner

Parameter	Value
Total areal density, g/m^2	200
Number of layers	3
Thickness, mm	3.26
Bulk density, kg/m^3	61
Porosity, %	95.5
Air permeability, cm^3/cm^2/s	138.89
Thermal resistance, m^{2}K/W	0.1136

2.2 Methods

To study the effect of the moisture percentage on the thermal liner's heat-protective performance, five moisture percentages (0, 25, 50, 75, and 100) were selected. The desired moisture content was achieved using a padding mangle. Samples were initially kept in a desiccator for 24 h, maintaining a temperature of 27 ± 2°C and 65 ± 2% relative humidity. Afterwards, the specimens were passed through the padding mangle to obtain the required expression. Post-padding, samples with the proper moisture percentages were maintained in an enclosed vessel sealed with paraffin tape and transported for heat-protective performance testing.

All samples were evaluated under three heat exposure conditions: 100% radiant, 50% radiant - 50% flame, and 100% flame. For each condition, samples were subjected to heat fluxes of 20 kW/m^2, 30 kW/m^2, and 40 kW/m^2). A total of 45 experiments were carried out, with HTI_{24} measured for each.

2.2.1 Testing Methods

HTI_{24} measurements were performed using a thermal protective performance (TPP) tester. The instrument was developed according to ASTM F 1939-15 standard. The samples were exposed to an incident heat flux in this device, and the backside temperature of the fabric was recorded with a copper calorimeter. Radiant heat was generated by a bank of five heating lamps, while flame heat was produced using two gas burners. For 50% radiant - 50% flame heat flux, both heating sources were used simultaneously. The temperature was measured by the copper calorimeter and sent to a computer via the ADAM processor. Figure 2 represents the instrument under different working conditions. To adjust the required heat flux, at first, at a certain level of input voltage and gas flow rate, the temperature was measured without the test samples. The heat flux was calculated using the following equation:

$$q = \frac{M.C_p.(Temp_{final} - Temp_{initial})}{absorptivity\,.A\,.(Time_{final} - Time_{initial})} \quad \ldots (1)$$

where M is the mass of the copper calorimeter; C_p, specific heat of copper; and A, the calorimeter's surface area.

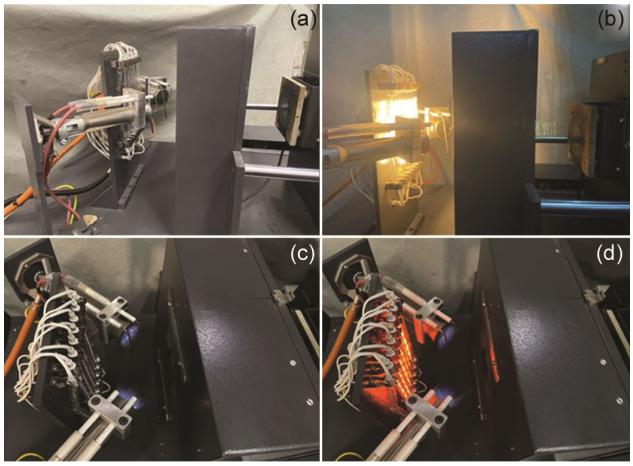

Fig. 2 — Testing instrument: (a) TPP tester, (b) radiant exposure, (c) flame exposure, and (d) 50 % radiant – 50 % flame exposure

After that, with the trial-and-error method, the specific input voltage and the gas flow rate were selected for all the heat fluxes. According to ISO 6942 (2022) and ISO 11613(2017) standards, HTI_{24} was the time required to achieve a 24℃ temperature rise in the calorimeter during the testing. HTI_{24} ranks the ability of materials and material assemblies to restrict heat energy transfer through the test material. ISO 9073-1:1989 standard procedure was followed to determine the areal density of the samples. INSTRON 3365 instrument was utilized to measure the thickness of the samples as per ISO 9073-2:1995. The bulk density of the specimens was calculated using the following equation:

$$\text{Bulk density of fabric } \left(\frac{\text{kg}}{\text{m}^3}\right) = \frac{\text{Areal density of the fabric } \left(\frac{\text{g}}{\text{m}^2}\right)}{\text{Thickness of the fabric (mm)}} \quad \ldots (2)$$

Based on their bulk density, the porosity of the samples was calculated using the following equation:

$$\text{Porosity (\%)} = \left(1 - \frac{\text{Bulk density (kg/m}^3)}{\text{Fibre density (kg/m}^3)}\right) \times 100 \quad \ldots (3)$$

A paramount air permeability master was used to measure the air permeability of the specimen according to ISO 9073-15:2007. KES-F7-II Thermolabo tester was utilized to measure the thermal resistance of the samples in accordance with ISO 5085-1:1989.

3 Results and Discussion

All test thermal liners are evaluated using a TPP tester and ranked based on the time required to reach a 24°C temperature rise on the backside of the liner. Table 2 presents the HTI_{24} values of the test samples with varying moisture percentages under different heat exposures.

3.1 Effect of Moisture Percentage at 20 kW/m^2 Heat Exposure

The HTI_{24} values of the test thermal liner at 20 kW/m² heat flux for radiant, flame, and 50% radiant–50% flame heat exposures are shown in Fig. 3. The results demonstrate that the HTI_{24} value consistently increases with the increase in moisture percentages

Table 2 — HTI_{24} values of the test samples

Heat flux, kW/m^2	20	30	40	20	30	40	20	30	40
Moisture percentage	50-50 flame and radiant			Flame			Radiant		
0	65	26	21	82	51	47	31	23	20
25	76	32	23	95	55	48	33	25	19
50	85	36	28	116	61	48	34	25	18
75	88	36	31	128	62	52	39	26	16
100	91	41	31	138	63	57	42	26	14

across all types of heat exposure. For flame exposure, the HTI_{24} value rises by 68 % as the moisture content increases from 0 % to 100 %, whereas the increase is 40 % and 35 % for 50 % radiant – 50 % flame and radiant heat exposure, respectively. This trend can be attributed to the higher specific heat of water than air, which requires more heat energy to raise the temperature, thereby delaying the time needed to achieve a 24℃ rise. Additionally, the increase in moisture content enhances the ablative effect, removing the thermal energy as latent heat from the surface of the test thermal liner. Similar trends are reported by various groups[9,10,12].

At 20 kW/m^2 heat flux, flame exposure yields the highest HTI_{24} for a given moisture percentage, while radiant exposure yields the lowest (Fig. 3). The HTI_{24} values increase as moisture content increases under every type of heat exposure. During flame exposure, the impinging flame generates a convective flow parallel to the fabric surface, reducing the heat flow through the fabric and increasing the time required to reach the calorimeter temperature rise of 24℃. In contrast, the thermal energy penetrates uniformly across the fabric's width under radiant heat exposure, resulting in faster heat transfer in less time and lower HTI_{24} values. The temperature rise of the calorimeter for the three heat exposure types at 20 kW/m² is shown in Fig. 4. During radiant exposure [Fig. 4 (a)], heat energy rapidly transfers through the fabric, causing a sharp increase in temperature. Under 50% radiant–50% flame exposure [Fig. 4 (b)], the heat transfer rate is intermediate, while in flame exposure [Fig. 4 (c)], the convective flow reduces the heat transfer rate. These findings align with observations by Lee and Barker[9].

3.2 Effect of Moisture Percentage at 30 kW/m^2 Heat Exposure

Figure 5 shows the effect of moisture percentage on the HTI_{24} at 30 kW/m^2 heat flux under radiant, flame, and 50 % radiant - 50 % flame heat exposures. HTI_{24} increases with rising moisture percentages for all exposure types. For 50 % radiant - 50 % flame exposure, HTI_{24} values exhibit a 50 % increment as the moisture percentage increases from 0 % to 100 %.

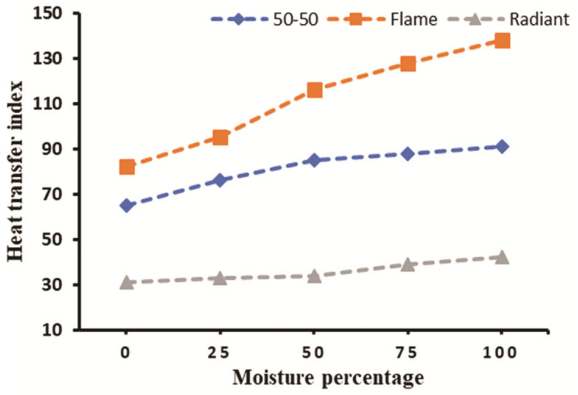

Fig. 3 — Effect of moisture percentage on the heat transfer index (HTI_{24}) of the test thermal liner at 20 kW/m^2 heat flux

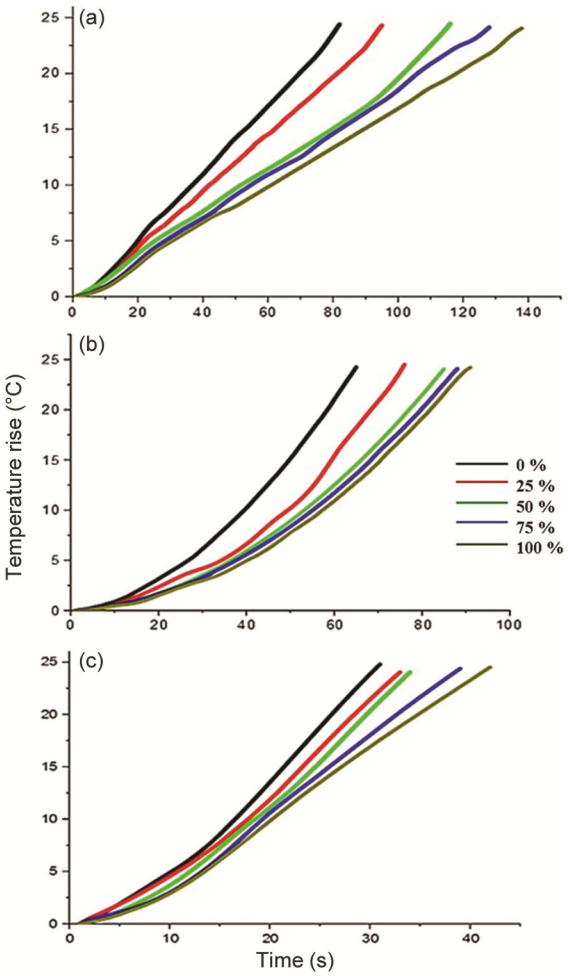

Fig. 4 — Temperature rise at 20 kW/m^2 heat flux during (a) radiant exposure, (b) 50 % radiant – 50 % flame exposure and (c) flame exposure

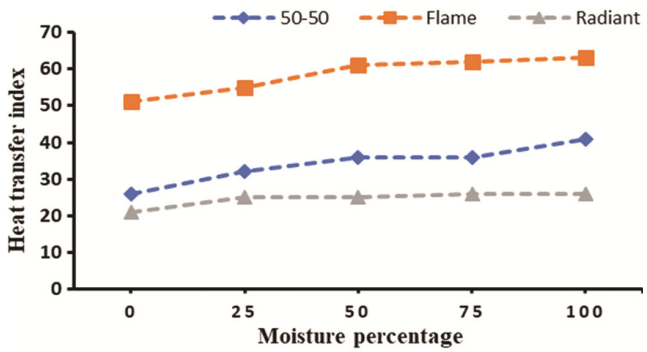

Fig. 5 — Effect of moisture percentage on the heat transfer index (HTI_{24}) of the test thermal liner at 30 kW/m^2 heat flux

In contrast, flame and radiant exposures show a 23% increase in HTI_{24} values. It is attributed to the higher specific heat of water than air, which necessitates greater heat energy to raise the temperature of the test specimen, resulting in higher HTI_{24} values. Figure 6 demonstrates the rise in temperature on the samples' back side over time. Flame exposure yields the highest HIT_{24} value, followed by 50 % radiant - 50 % flame and radian exposure. This difference is likely due to the penetrating nature of radiant heat, which traverses the entire fabric thickness, leading to a faster temperature rise on the back side, and consequently, lower HTI_{24} values. These findings align with the patterns reported in earlier studies[9,30].

3.3 Effect of Moisture Percentage at 40 kW/m^2 Heat Exposure

Figure 7 demonstrates the HTI_{24} values for three heat exposures. Flame and 50% radiant–50% flame exposures consistently increase HTI_{24} value with the rising moisture levels. The same kind of trend can be found for both 20 kW/m^2 and 30 kW/m^2 heat flux. However, at radiant heat exposure, HTI_{24} decreases by 30 % as moisture content increases from 0 % to 100 %. It is attributed to moisture vaporization, which enhances the fabric's heat transfer efficiency, increasing the backside temperature and resulting in a lower HTI_{24} value. Figure 8 shows the temperature rise trends, similar to those observed at 20 kW/m² and 30 kW/m². These findings align with the work of Lee and Barker[9].

3.4 Effect of Moisture in Radiant Exposure

Table 2 indicates that moisture positively influences HTI_{24} at 20 kW/m^2 and 30 kW/m^2, but negatively affects it at 40 kW/m² under radiant exposure. An analysis of variance (ANOVA) study examines the effect of moisture percentage and incident heat flux. The regression equation for radiant heat exposure is given below:

$$HTI = 52.33 + 0.027 \times Moisture\ percentage - 0.92 \times Heat\ flux \quad \ldots (4)$$

R^2 value of 0.8891 and a low p-value of 1.8569e^{-06} indicate the goodness of fit of the model (Table 3).

3.5 Effect of Moisture in 50 % Radiant - 50 % Flame Exposure

Table 2 shows the HTI_{24} value of the test samples under 50 % radiant - 50 % flame exposure at different heat flux and moisture percentages. For every heat flux level, moisture has a beneficial impact on the HTI_{24} value, while the heat flux has a devastating effect. The regression equation for this condition is as follows:

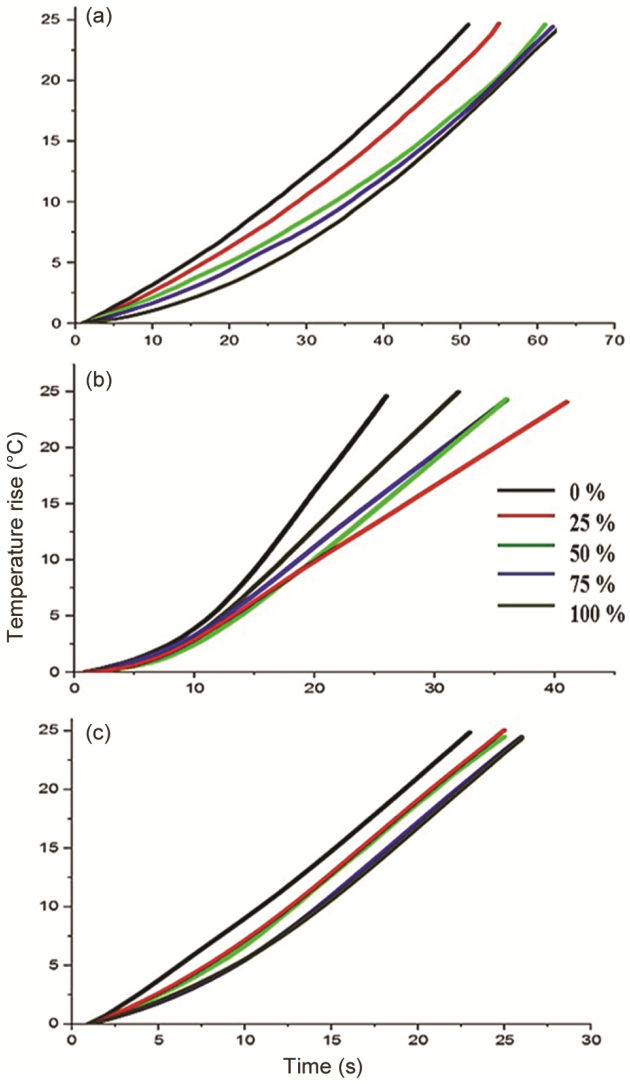

Fig. 6 — Temperature rise of the calorimeter at 30 kW/m^2 heat flux during (a) radiant exposure, (b) 50 % radiant – 50 % flame exposure and (c) flame exposure

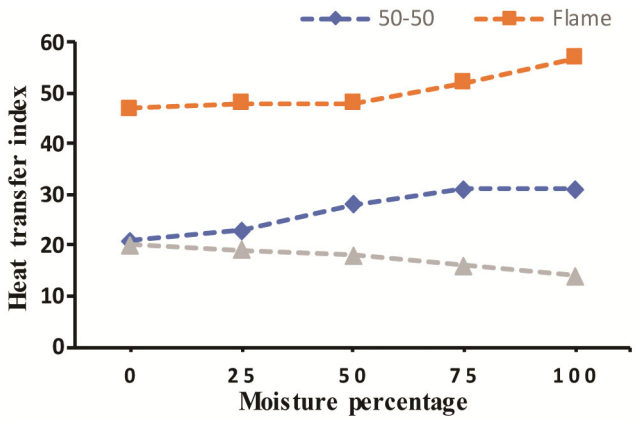

Fig. 7 — Effect of moisture percentage on the heat transfer index (HTI_{24}) of the test thermal liner at 40 kW/m^2 heat flux

Table 3 — ANOVA results

		Radiant heat exposure			
	df	SS	MS	F	p-value
Regression	2	859.7333	429.8667	48.1194	1.8569E^{-06}
Residual	12	107.2	8.933333		
Total	14	966.9333			
		50 % radiant - 50 % flame exposure			
	df	SS	MS	F	p-value
Regression	2	7873.3	3936.65	33.26668	1.27E^{-05}
Residual	12	1420.0333	118.3361		
Total	14	9293.3333			
		Flame exposure			
	df	SS	MS	F	P value
Regression	2	10758.23	5379.117	23.92934	6.49E^{-05}
Residual	12	2697.5	224.7917		
Total	14	13455.73			

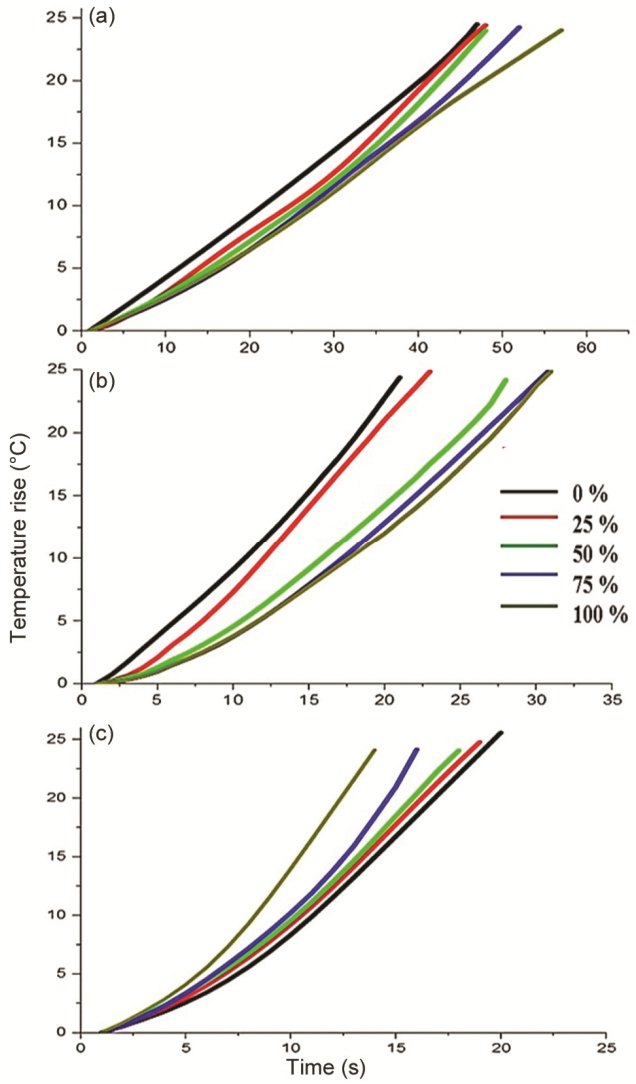

Fig. 8 —Temperature rise of the calorimeter at 40 kW/m^2 heat flux during. (a) radiant exposure, (b) 50 % radiant – 50 % flame exposure and (c) flame exposure

$$HTI_{24} = 120.23 + 0.168 \times Moisture\ percentage - 2.71 \times Heat\ flux \quad \ldots(5)$$

The higher R^2 value of 0.8471 and lower p-value of 1.27e^{-05} exhibit the excellent fitness of the model (Table 3).

3.6 Effect of Moisture in Flame Exposure

Table 2 outlines the HTI_{24} values under flame exposure at varying moisture percentages and heat fluxes. HTI_{24} decreases with increasing heat flux for any moisture level but increases with moisture content for any given heat flux. Table 3 shows the ANOVA results for flame exposure, and the regression equation to predict the HTI_{24} value at different heat flux and moisture content is given below:

$$HTI_{24} = 152.3 + 0.267 \times Moisture\ percentage - 3.07 \times Heat\ flux\ - 2.71 \times Heat\ flux \quad \ldots(6)$$

The R^2 value of 0.7995 and low p-value of 6.49e^{-05} show the fitting of the model (Table 3).

4 Conclusion

The study demonstrates that moisture content significantly impacts the thermal performance of fire-protective clothing under varying heat exposures. The test results indicate that the effect of moisture on the heat protective performance of a multi-layer thermal liner is complex. At a lower heat flux, the moisture acts positively under every kind of heat exposure and increases the protection level. However, at higher heat flux under flame exposure and 50 % radiant - 50 % flame exposure, the protection time increases as the moisture level rises, while during radiant exposure, the protection time decreases with the water level. On the contrary, for every kind of heat exposure and

every level of moisture percentage, the HTI_{24} value decreases as the incident heat flux increases. The regression models and ANOVA analyses confirm the significant interplay of moisture content and heat flux on HTI_{24} values, with high R^2 values indicating strong model reliability. These findings provide valuable insights into optimizing fire-protective clothing by leveraging moisture content to enhance thermal performance under specific exposure conditions.

Acknowledgements

This work was supported by the Defence Research and Development Organisation (DRDO), Ministry of Defence, Govt. of India (Project code- RP03456).

References

1 Hall S & Evarts B, *Fire Loss in the United States During, (NFPA ®) Key Findings*, (2022).
2 Lawson J R, Fire F, Stull, J O & Schwope A D, (Eds) *Performance of Protective Clothing*, ASTM STP, (1997) 334.
3 Keiser C, Becker C & Rossi R M, *Text Res J*, 78 (2008) 604.
4 Keiser C & Rossi R M, *Text Res J*, 78 (2008) 1025.
5 Lawson J R, Fire Fighter's *NISTIR 5804, National Institute of Standards and Technology*, (1996) 1.
6 Bajaj P & Sengupta A K, *Protective Clothing*, Textile Institute, (1992).
7 Makinen H, Fire fighter's, Protective Clothing, in *Textiles for Protection*, (2005) 622.
8 Rossi R, 'Interactions between Protection and Thermal Comfort', in Scott, R.A. (Edn) *Textiles for Protection*, Woodhead Publishing Limited, (2005) 233.
9 Lee Y M & Barker R L, *J Fire Sci*, 4 (1986) 315.
10 Barker R L, Guerth-Schacher C, Grimes R V & Hamouda H, *Text Res J*, 76 (2006) 27.
11 Lu Y, Li J, Li X & Song G, *J Fire Sci*, 31 (2013) 99.
12 Rathour R, Rajput B, Das A & Alagirusamy R, *J Text Inst*, 114 (2022) 1682.
13 Fu M, Weng W G & Yuan H Y, *J Hazard Mater*, 276 (2014) 383.
14 Barnes P, *J Hazard Mater*, 86 (2001) 25.
15 Han Z Y & Weng W G, *J Hazard Mater*, 189 (2011) 509.
16 Tao C, He Y, Li Y & Wang X, *J Hazard Mater*, 260 (2013) 552.
17 Karter M J, *Fire Loss In The United States During 2013, Fire Loss In The United States During,* Quincy. (2014)
18 Butler B W, *6th Int Conf Forest Fire Res*, (2010) CD-ROM.
19 Luo M & Beck V, *Fire Saf J*, 26 (1996) 191.
20 Ierardi J A, A Computer Model of Fire Spread from Engine to Passenger Compartments in Post-Collision, (May) (1999).
21 Barker R, *A Review Of Gaps And Limitations In Test Methods For First Responder Protective Clothing And Equipment*. (2005). Available At: http://www.cdc.gov/niosh/npptl/pdfs/protclothequipreview.pdf.
22 Foster J & Roberts G V, (*Measurements of the Firefighting Environment*, *Central Fire Brigades Advisory Council Scottish Central Fire Brigades Advisory Council Joint Committee on Fire Research*, (1994).
23 Hoschke B N, *J Clothing*, 4 (1981) 125.
24 Abbott N J & Schulman S, *J Coat Fabr*, 6 (1976) 48.
25 Kothari V K & Chakraborty S, *Fibers Polym*, 17 (2016) 809.
26 Das T, Das A & Alagirusamy R, *J Ind Text*, (2022) 1
27 Barker R L & Young M L, *Text Res J*, 57 (1987) 331.
28 Kukuck S, *Thermal Performance of Fire Fighters' Protective Clothing. 3. Simulating a TPP Test for Single-Layered Fabrics*. Gaithersburg, (2003).
29 Udayraj & Wang F, *Int J Therm Sci*, 130 (2018) 28.
30 Rajput B, Rajput B, Rathour R, Das T, Ray B, Das A & Talukdar P, *J Text Inst*, 115 (2022) 218.